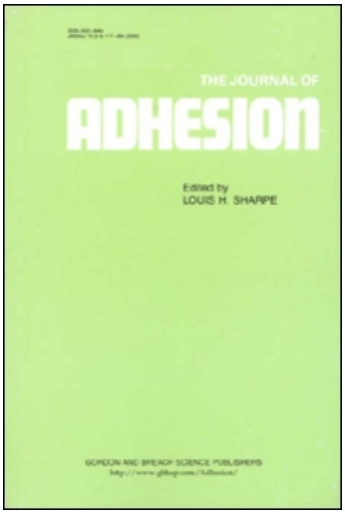


## The Journal of Adhesion

Publication details, including instructions for authors and subscription information:
http://www.informaworld.com/smpp/title~content=t713453635

# Adhesion Properties of Lightly Crosslinked Solvent-Swollen Polymer Gels

Joseph L. Lenhart[a]; Phillip J. Cole[a]
[a] Sandia National Laboratories, Albuquerque, New Mexico, USA

**To cite this Article** Lenhart, Joseph L. and Cole, Phillip J.(2006) 'Adhesion Properties of Lightly Crosslinked Solvent-Swollen Polymer Gels', The Journal of Adhesion, 82: 10, 945 — 971
**To link to this Article: DOI:** 10.1080/00218460600875953
**URL:** http://dx.doi.org/10.1080/00218460600875953

*The Journal of Adhesion*, 82:945–971, 2006

ISSN: 0021-8464 print/1545-5823 online
DOI: 10.1080/00218460600875953

Taylor & Francis
Taylor & Francis Group

# Adhesion Properties of Lightly Crosslinked Solvent-Swollen Polymer Gels

**Joseph L. Lenhart**
**Phillip J. Cole**
Sandia National Laboratories, Albuquerque, New Mexico, USA

*Polymer gels are crosslinked polymer networks, highly swollen with solvent. For practical gel applications adhesion to a wide range of substrates over a broad range of temperatures is desired. In this article the adhesive properties of two types of solvent-swollen elastomers were studied, utilizing a combination of tack, contact mechanics, and peel adhesion methods. The first gel was a crosslinked polybutadiene swollen with common polymer plasticizers, while the second was a commercially available silicone with high extractables content. Nominally, these solvent-swollen materials exhibit similar adhesive characteristics to nonsolvent swollen elastomers including: (1) an increase in tack adhesion energies with increasing pull-off rates and decreasing temperatures in the rubbery region, (2) qualitative correlation between the rheological loss tangent for the gel and the gel adhesion energy, (3) fibrillation and extension during adhesion testing for gels with a shear modulus value less than $10^5$ Pa in the plateau region, and (4) a decrease in the adhesion energy with increasing crosslink density. However, the presence of solvent in the elastomer can lead to solvent exclusion effects that degrade tack adhesion and must be considered for gel design in practical applications.*



**Keywords:** Adhesion; Elastomer; Gel; Silicone; Swelling; Tack

## INTRODUCTION

Polymer adhesion to a variety of surfaces is critical to a broad range of technological applications including microelectronics, rubber

Received 28 November 2005; in final form 18 May 2006.
One of a Collection of papers honoring Hugh R. Brown, who received *The Adhesion Society Award for Excellence in Adhesion Science, Sponsored by 3M* in February 2006.
Address correspondence to either Phillip J. Cole, Organic Materials Department, Org. 2453, Sandia National Laboratories, P.O. Box 5800, MS 1245, Albuquerque, NM 87185, USA. E-mail: pjcole@sandia.gov or Joseph L. Lenhart, Organic Materials Department, Org. 1821, Sandia National Laboratories, P.O. Box 5800, MS 0888, Albuquerque, NM 87185, USA. E-mail: jllenha@sandia.gov

technology, biomaterials, etc. Due to this broad technical importance, significant effort has been devoted to investigating the mechanisms of polymer adhesion. For example, with polymer adhesion to substrates it is well-known that surface treatments such as surface roughening, various types of cleaning, and chemical coupling agents can increase the strength of a polymer adhesive bond to a substrate [1]. For polymer-polymer adhesion an important mechanism is the interpenetration of polymer chains across the interface [2].

In glassy polymers interpenetration can be generated by heating the polymers above the glass transition temperature, increasing chain mobility, and allowing polymer-polymer interdiffusion to strengthen that interface. This is a process called "welding." The extent of interpenetration, or the interfacial width, plays a dramatic role in the interface strength [3,4]. Interfacial toughness has been shown to remain low until the interfacial width becomes larger than the entanglement length of the polymer chains. The interfacial toughness then increases substantially until the interfacial width approaches several times the entanglement length [3]. For incompatible polymers in which the interfacial width is small, adhesion can be enhanced through the addition of a diblock or random copolymer. The segregation of an A-B copolymer to the interface, in which the A-type monomer is soluble in one polymer and the B-type monomer is soluble in the other, effectively stitches the interface together and increases its strength [5–7].

For elastomer-substrate and elastomer-elastomer adhesion chain entanglement at the interface can also enhance the adhesion [8,9]. However, with elastomers bulk energy dissipation also plays a major role, leading to viscoelastic dissipation in a large region around the crack tip. These viscoelastic losses lead to strong rate and temperature dependencies of the interfacial toughness for elastomer adhesion that can be described through the following generalized expression [10,11]:

$$G(R) = G_o[1 + f(a_t R)] \tag{1}$$

where G(R) is the rate dependent interfacial toughness, $G_o$ is the limiting toughness at zero rate, R is the crack velocity, and $a_t$ is the shift factor from the WLF equation [12].

Our interest is in the properties of extremely soft materials, specifically polymer gels. A polymer gel is a physically or chemically crosslinked polymer that is highly swollen by solvent. Mechanically, the solvent creates a "soft solid" that is easily deformable, yet still recovers from the deformation due to the elastic nature of the crosslinks in the polymer [13]. Polymer gels offer potential in a wide array of applications because the gel properties can be tuned by varying the polymer

type, solvent type, and solvent loading. In addition, small molecule additives and fillers can be incorporated into the gel formulation to further enhance the properties. Polymer gels have been studied for many years [14–16] and early work focused on potential electro-active applications in which mechanical motion can be induced in the gel through an applied electric field [17,18]. Recently, gels are emerging for consideration in a range of practical applications from biomedical technology [19–22] to electronic devices [23–25].

For gel design and implementation adhesion to a variety of different substrates is critical for performance in practical applications. The purpose of this article is to outline our recent work, which is focused on understanding the role of the solvent in the polymer gel on the adhesive properties. Several different types of adhesion measurements have been heavily utilized for characterizing adhesion with soft materials including peel, tack adhesion, and JKR contact mechanics [26–31]. Through these tools, we have been able to probe solvent issues in polymer gels.



## EXPERIMENTAL

### Materials

Two types of polybutadiene monomers were used to form the crosslinked network, including one containing maleic anhydride (MA) functional groups (MA10 or MA5) and the other containing hydroxyl (OH) groups (R45). The hydroxyl groups react with the maleic anhydride groups to form ester crosslinks. The crosslinking reaction is performed in the presence of solvent. The major solvents utilized were dibutylphthalate (DBP) and bis(ethylhexyl)sebacate (BEHS). A catalyst, didecylmethylamine, promoted the crosslinking reaction. The gels were cured at 75°C for 6 days. Rheological measurements confirmed that 6 days at 75°C resulted in a fully cured gel material because the plateau modulus was unchanged at longer times. The cured gels had an extractable content equal to the solvent loading plus 2 to 3 mass % of unreacted polymer precursors. The maleic anhydride and hydroxyl-functionalized polybutadienes were used as received from the Sartomer Company (Exton, PA, USA). The solvents were used as received from Aldrich (Milwaukee, WI, USA). The monomers utilized in this study were commercial grade materials, leading to imperfections in the gel structure such as dangling chain ends that can enhance adhesion performance when compared with ideal, endlinked gels. The role of these imperfections on the adhesive properties will be discussed in the Results and Discussion section.

## Rheological Characterization

Rheological measurements were made with rectangular gel samples in a torsion geometry. The gel samples had dimensions of approximately $12 \times 4.5 \times 28$ mm. The measurements were made on a Rheometric Scientific ARES instrument (TAInstruments, New Castle, DE, USA) at a frequency of 1 Hz and a scan rate of 2°C/min. An environmentally controlled chamber permitted determination of the modulus over temperatures from –100 to 70°C. Strain sweeps were conducted at various temperatures to ensure that the modulus was independent of strain.

## Tack Adhesion

Tack adhesion measurements were made by curing the polybutadiene gel in a thin film (~0.5 mm thick) on an aluminum plate. A stainless steel cylindrical punch (8 mm diameter) was brought into contact with the gel film and held for 60 s at a force of 500 g. The probe was pulled away from the gel film at a controlled rate, while measuring the force-displacement curve. The temperature for the tack measurement was held constant utilizing an environmental chamber. The sample was allowed to equilibrate at the measurement temperature for 10 to 15 min prior to each measurement. To get an effective tack adhesion energy the stress (force/probe area)-strain (displacement/film thickness) curve was integrated, multiplied by the gel sample thickness, and given a Poisson's ratio correction by multiplying by $1 - \nu^2$, where $\nu$ is 0.5 for a rubbery polymer.



## Peel Adhesion

Peel adhesion measurements at various rates and temperatures were made with silicone gels sandwiched between either aluminum or Mylar® substrates. The peel angle was 90° and the peel temperature was controlled by an environmental chamber with liquid nitrogen cooling capability. To eliminate variations in the substrate properties and allow direct comparison between peel on the two different substrates a Mylar-aluminum laminate substrate was utilized.

# RESULTS AND DISCUSSION

## Rheology of Solvent Swollen Polybutadiene Gels

Figure 1 shows the primary constituents of the gel formulation. The gel is composed of two monomers. One is a polybutadiene oligomer

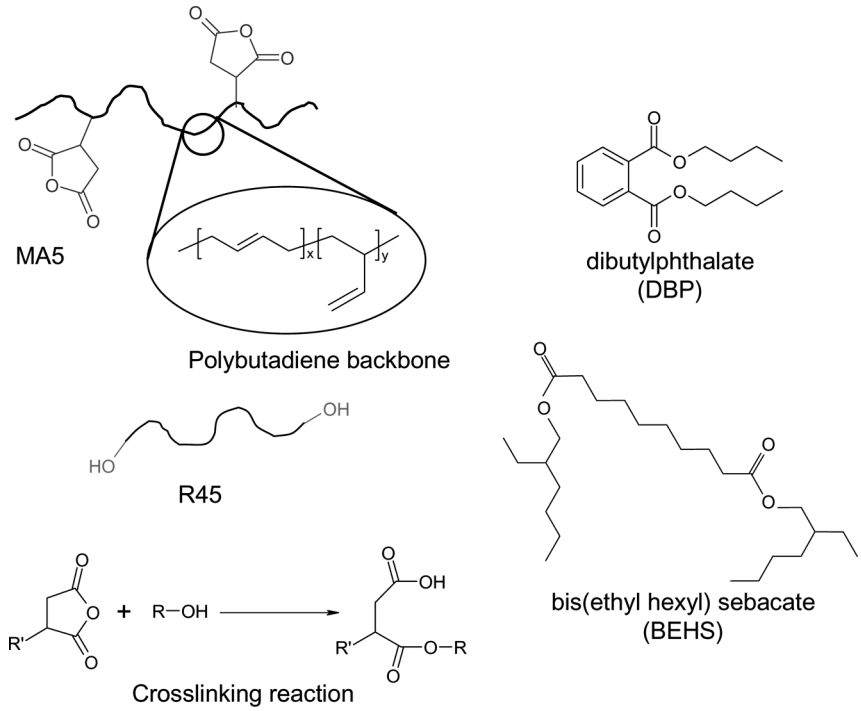


**FIGURE 1** The primary constituents of the gel formulation are shown, as well as the crosslinking reaction.



with maleic anhydride groups grafted to the backbone and is referred to as MA5 ($M_n \sim 5300\,g\,mol^{-1}$, an average of $\sim 2.5$ maleic anhydride groups per polymer chain, polydispersity index $\sim 2.5$) [32]. In some cases the MA5 oligomer is replaced with an MA10 oligomer, in which the average functionality is doubled (*i.e.*, $\sim 5$ maleic anhydride groups per chain). The other component of the polybutadiene networks has hydroxyl functional groups and is referred to as R45 ($M_n \sim 2800\,g\,mol^{-1}$, an average of $\sim 2.5$ hydroxyl groups per polymer chain, polydispersity index $\sim 2.5$) [32]. Polybutadiene is a flexible polymer chain with a $T_g$ near $-85^{\circ}C$ [33]. The low functionality of the monomers ensures a loosely crosslinked gel with a low glass transition temperature and a low rubbery modulus. The maleic anhydride functionality on MA5 or MA10 reacts with the hydroxyl functionality on R45 to form an ester linkage (reaction schematic shown in Figure 1). The crosslinking reaction is promoted with a small fraction, $\sim 0.5$ mass%, of a tertiary amine catalyst, didecylmethylamine. Two low volatility polymer

plasticizers, dibutylphthalate (DBP) and bis(ethylhexyl)sebacate (BEHS), were utilized as the solvent.

To assess the impact of crosslink density on the gel rheology and adhesion three gel formulations were studied. The first was a stoichiometric formulation (equal number of maleic anhydride and hydroxyl groups) of MA10 and R45 with 60 mass% BEHS. The second was a stoichiometric formulation of MA5 and R45 with 60 mass% BEHS. The third was an off-stoichiometric formulation (in this case with 40% excess hydroxyl groups relative to maleic anhydride groups) of MA5 and R45 with 60 mass% BEHS. Figure 2a plots the elastic component of the shear modulus, G′, as a function of temperature for these gel formulations. The glass transition temperature ($T_g$) (as defined by the peak in the loss tangent, Figure 2b) is similar for all three gel formulations at approximately $-80^{\circ}C$, indicating that the crosslink density is low, and the $T_g$ is dominated by the polybutadiene backbone between the crosslinking junctions. As expected, the plateau value for the rubbery modulus of the MA10 gel is highest, nearly an order of magnitude higher than the value for the stoichiometric MA5 gel. This is due to the higher maleic anhydride functionality on MA10 and the resulting higher crosslink density. The MA5 gel with 40% excess hydroxyl groups has the lowest value of the



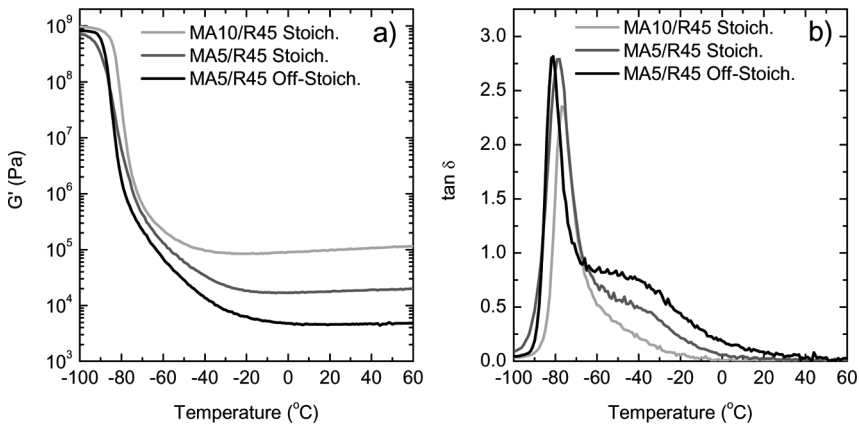


**FIGURE 2** a) Storage (Elastic) modulus as a function of temperature for a stoichiometric MA10/R45 gel, a stoichiometric MA5/R45 gel, and an off-stoichiometric MA5/R45 gel with 40% excess hydroxyl groups. All gels had 60 mass% BEHS. b) Loss tangent as a function of temperature for the same gel formulations. The relative uncertainty in the modulus values is less than $\pm 10\%$, as was demonstrated by measurements on multiple samples of each gel formulation.

rubbery modulus due to the reduced crosslink density in the off-stoichiometric formulation. An important consideration for utilizing gels in various applications is maintaining adequate adhesion over a broad range of operating temperatures. Rheological characterization of these gels can provide qualitative insight into their adhesive capabilities. For example, with pressure sensitive adhesives it was observed that tack adhesion deteriorates when the rubbery shear modulus exceeded a value of $10^5$ Pa (Dalquist criterion) [34]. Since the MA10-based gel has a rubbery modulus near this value, it is likely to exhibit poor tack adhesion. Both the MA5 stoichiometric and off-stoichiometric formulations should exhibit higher tack adhesion due to the lower rubbery shear modulus values.

Figure 2b shows the loss tangent, $\tan\delta$, (shear loss modulus/shear storage modulus) for the same gel formulations. The loss tangent represents the ability of a system to dissipate energy, and can be qualitatively correlated with the tack adhesion energy. For the three gel formulations the loss tangent spectra are similar, except in the region between $-10$ and $-70$°C. In that region the loss tangent is lowest for the MA10 stoichiometric gel, intermediate for the MA5 stoichiometric gel, and highest for the MA5 off-stoichiometric formulation. This enhanced energy dissipation combined with a lower rubbery modulus value will enhance the adhesive performance of the MA5 gels compared with the MA10 gels. Through investigation of the loss tangent spectra, one would expect the low temperature tack adhesion for the MA5 off-stoichiometric gel to be the highest and the tack adhesion of the MA10 stoichiometric gel to be lowest. While the molecular origin of the enhanced loss tangent between $-10$ and $-70$°C for the MA5 based formulations is unclear, it may be due to the presence of pendant chain defects in the gel structure. The amount of these defects will increase with the decrease in monomer functionality and the off-stoichiometric formulations.



## Tack Adhesion of Solvent Swollen Polybutadiene Gels

In polymer gel applications adhesion to a wide array of substrates over a broad range of temperatures is critical. For soft materials like these gels adhesion is dictated by two factors. First is the ability of the soft material to conform to a substrate and obtain intimate contact. If the gel is cured in the presence of the substrate, then intimate contact is determined by the ability of the gel material to wet the surface. If the gel is brought into contact with the substrate after cure, then the contact pressure, contact time, surface roughness, and flexibility of the gel material can play a significant role, in addition to the

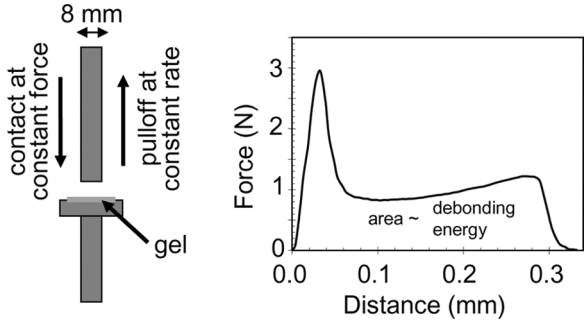


**FIGURE 3** A schematic of the tack adhesion testing procedure as well as a typical force-displacement curve.



interaction between the gel and the substrate surface [31,34–37]. A second and equally important factor for adhesion with soft materials is the ability of the bulk gel material to dissipate energy. In addition to the rheological loss tangent data in Figure 2, tack adhesion measurements are an ideal tool to quantify this energy dissipation ability [2,10,11]. Figure 3 shows a schematic of the tack adhesion measurement. A thin gel layer ($\sim$0.4 mm thick) is cast on a disposable aluminum plate. The face of a small cylindrical stainless steel probe (8-mm diameter) is brought into contact with the gel surface, and held in contact at a constant force of 500 g for 60 s. This hold time is long enough to allow intimate contact between the gel and the metal probe surface. The stainless steel probe is then pulled away from the gel at a constant rate, while measuring the pull-off force and displacement.

A schematic of a typical pull-off force *versus* displacement curve is also shown in Figure 3. The force is typically normalized with the contact area of the probe, while the displacement is normalized with the gel film thickness to obtain a stress-strain diagram. The shape of the stress-strain diagram, as well as the area under the stress-strain curve (effective tack adhesion energy or practical work of adhesion, $W_{adh}$), provide insight about adhesion and energy dissipation in soft materials.

Figure 4a–c shows typical stress-strain plots for tack adhesion measurements of the MA10 stoichiometric, MA5 stoichiometric, and MA5 off-stoichiometric formulations, respectively, at temperatures of 24, $-30$, and $-60^{\circ}$C and at a pull off rate of 0.02 mm/s. The tack adhesion energy is defined as the integral of the stress-strain curve from zero displacement to complete adhesive pull-off. For each formulation the tack adhesion energy increases with decreasing measurement

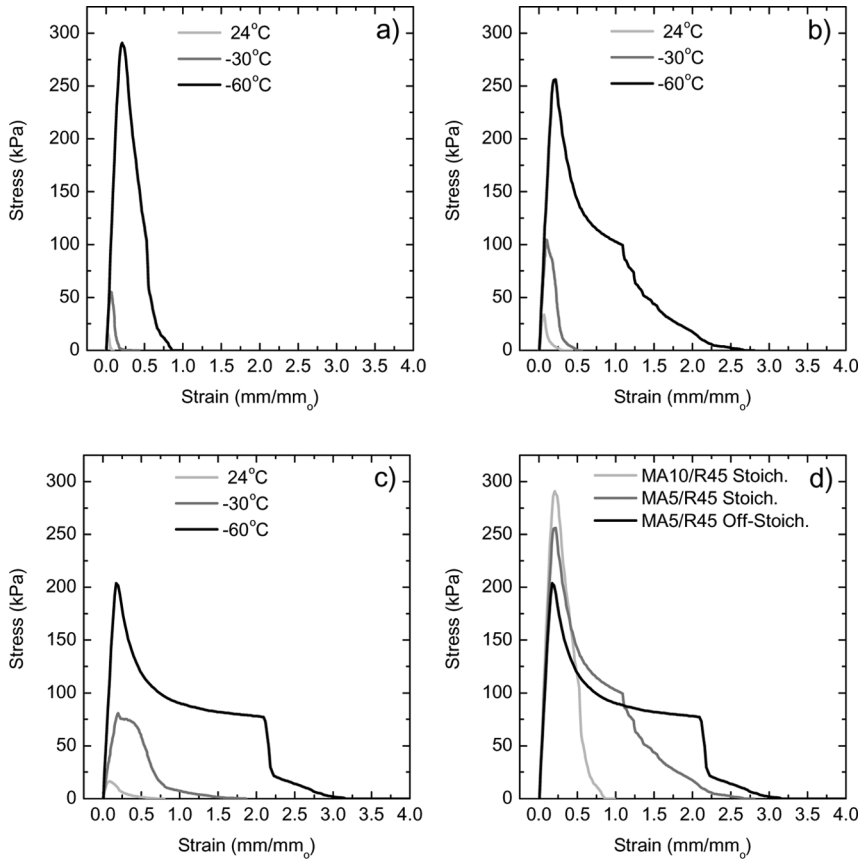


**FIGURE 4** Tack adhesion stress-strain curves as a function of temperature for a) MA10/R45 stoichiometric, b) MA5/R45 stoichiometric, and c) MA5/R45 off-stoichiometric formulations. d) Stress-strain curves for the three formulations at $-60^{\circ}$C. All curves are shown for a rate of 0.02 mm/s.

temperature. This is a combined effect from an increase in the maximum stress as well as an increase in the strain at final pull-off with decreasing temperature, and is due to the increase in the loss tangent at lower temperatures leading to enhanced energy dissipation during pull-off. For elastomeric adhesives, both the peel force and tack adhesion energy will increase with decreasing temperature and increasing rate, as the adhesive properties are driven into a regime in which energy dissipation is high. Eventually, at still lower temperatures and faster rates, the adhesion will decrease rapidly as the adhesive becomes glassy and loses its energy dissipating capabilities

[28]. In all cases, the failure locus was adhesive failure at the gel-probe interface. The solvent-swollen polymer gels behave similarly to pressure-sensitive and other elastomeric adhesives.

The highest crosslink density formulation (MA10/R45 stoichiometric) fails like an elastic rubber at all temperatures with small strain values at final pull-off. This is the type of failure mechanism observed in pressure-sensitive adhesives with plateau moduli near $10^5$ Pa or higher [37]. This nondissipative type of failure can also be observed in lower modulus loosely crosslinked adhesives at low temperatures and fast rates as the adhesive approaches the glassy regime and the failure becomes brittle [28,38]. This failure was not observed for the MA5 formulations because the measurements were not made at low enough temperatures or fast enough rates to invoke this failure response. The MA5 gels both exhibit larger extension in the stress-strain diagram than the MA10-based gel, which is consistent with the lower crosslink densities of these formulations. The MA5 off-stoichiometric formulation exhibits the largest extension at all temperatures. At $-60^{\circ}$C the MA5 off-stoichiometric formulation exhibits dramatic extension, which is due to the formation of fibrils that grow and extend during the adhesion test, providing an energy dissipation mechanism [29–31].



Figure 4d compares the MA10 stoichiometric, MA5 stoichiometric, and MA5 off-stoichiometric data at $-60^{\circ}$C and a rate of 0.02 mm/s, in which the gels are in a regime where the energy dissipation is high. The maximum pull-off stress increases with increasing gel crosslink density. This is because the maximum pull-off force is associated with the onset of cavitation near the probe-gel interface [39]. The energy required to generate this cavitation will increase with increasing crosslink density and shear storage modulus value in the plateau region [39]. The MA10 gel fails like an elastic adhesive with minimal energy dissipation, in which the stress rises sharply with initial strain, reaches a maximum, and then decreases sharply as the gel snaps away from the probe surface. The MA5 stoichiometric formulation exhibits a similar rapid rise in stress with increasing strain. The onset of cavitation occurs at a lower stress value due to the lower modulus of the system. After the maximum, the stress drops with increasing strain, but exhibits an extension in the stress-strain diagram before the gel pulls away gradually from the probe surface. This extension in the stress-strain diagram has been studied extensively [29–31,39–41]. The tack adhesion involves three basic deformation mechanisms. The first is cavitation near the gel-probe interface or in the bulk film. Cavitation results in the rapid rise and fall of the stress at low strains and precedes the second two deformation processes. The

next mechanisms are lateral and normal cavity growth, which can occur either in sequence or simultaneously. Normal cavity growth leads to the fibrillar structures and large extension commonly observed in tack testing. The formation of these fibrils was directly observed for both the MA5 stoichiometric and MA5 off-stoichiometric formulations through the side view window in the rheometer. For the MA5 off-stoichiometric formulation the maximum in the stress-strain curves are the lowest of the formulations, but the fibrillation was the most extensive, the strain at final pull-off was the largest, and the gel snaps away from the probe surface abruptly, presumably as the fibrils generate enough force to cause the gel to delaminate from the probe. This energy dissipation process that occurs for the MA5 off-stoichiometric formulation is consistent with the high loss tangent values for the off-stoichiometric formulation at $-60^{\circ}$C. For pressure-sensitive adhesives loss tangent values above 0.2 led to high tack adhesion energies and extension/fibrillation during the tack measurement [41]. At $-30^{\circ}$C and $-60^{\circ}$C both MA5 formulations have loss tangent values significantly greater than 0.2, explaining the large extensions.



Figure 5a, b, and c plot the tack adhesion energy (area under the stress-strain curve) as a function of rate at the three measurement temperatures for the MA10 stoichiometric, MA5 stoichiometric, and MA5 off-stoichiometric formulations, respectively. The figures are shown on the same scale for comparison. At 24°C no significant rate dependence was observed for any of the gel formulations. At both $-30$ and $-60^{\circ}$C strong rate dependence was observed, which is consistent with the increase in the loss behavior at the lower temperatures. The

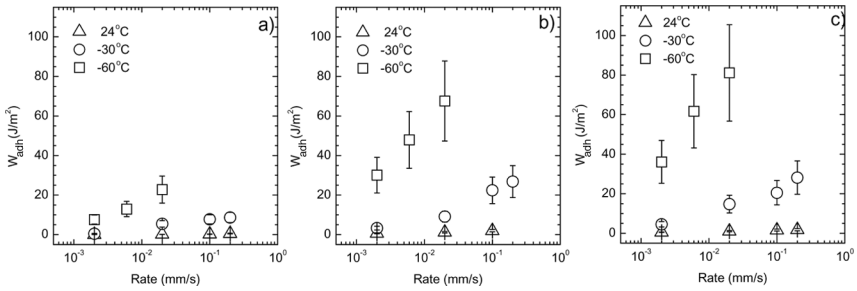


**FIGURE 5** Tack adhesion energy (practical work of adhesion, $W_{adh}$) as a function of rate at temperatures of 24, $-30$, and $-60^{\circ}$C for a) MA10/R45 stoichiometric, b) MA5/R45 stoichiometric, and c) MA5/R45 off-stoichiometric formulations.

rate dependence also increases with decreasing temperature for all three formulations. The high crosslink density MA10 formulation exhibits the lowest tack adhesion energies at all temperatures and rates. This is due to the lack of fibrillation during probe pull-off and the nondissipative type of failure in the tack adhesion measurement. Interestingly, the MA5 off-stoichiometric gel formulation shows similar tack adhesion energies to the MA5 stoichiometric formulation, despite the larger extension and fibrillation for the MA5 off-stoichiometric formulation. This is because the lower maximum in the stress-strain curve for the MA5 off-stoichiometric formulation offsets the larger extension (see Figure 4d). It is important to note that the fibrils that form during extension likely lead to a reduction in the actual contact area between the probe and gel, or as the fibrils extend and become thinner, a decrease in the effective area over which the force is acting on the gel. This decrease in effective area with fibrillation skews the tack measurement towards lower calculated stress. Accounting for these area changes during the tack measurement would lead to the true stress and the real energy required to separate the probe and gel. This requires visual observation of the contact area during the tack measurement which has been pursued by a number of research groups [28–31,39–41]. We are currently building an instrument that will allow this type of inspection. For our gel applications gel tack adhesion has been correlated with performance in a variety of devices. Qualitatively, gels that exhibit fibrillation and extension during the tack adhesion testing at low temperatures have performed well in devices, while gels that exhibit a nondissipative type of failure like the MA10 formulation have performed poorly. Therefore, in our case the qualitative shape of the stress-strain curve and the observation of extension and fibrillation were a clear indicator of gel performance in practical applications.

It is important to discuss the molecular mechanisms of energy dissipation that occur during the tack measurements and how the solvent can potentially add new dissipation phenomena. Obviously, chain stretching and friction can contribute to energy dissipation. In addition the presence of dangling chain ends (especially in the off-stoichiometric formulation) can lead to chain pull-out effects during the cavitation and fibrillation process. Chain pull-out is a common energy dissipating mechanism for elastomer-elastomer interfaces, and crack propagation through elastomers [8,9]. Because these gels are not model formulations formed by controlled endlinking dangling end defects are likely present even in the stoichiometric formulations and will contribute to energy dissipation during adhesion measurements. In addition, because the

gel is crosslinked chemical bonds must also break during cavitation and fibrillation, which will dissipate energy. Physical mechanisms of energy dissipation have also been proposed. For example, during the cavitation process voids can form at the adhesive-probe interface leading to a "suction-cup" effect which increases the pull-off force [42]. These molecular energy dissipation mechanisms are present in both solvent-swollen and nonsolvent swollen elastomers. However, in solvent-swollen elastomers the presence of solvent at the interface, microstructural variations in the gel due to the solvent loading and phase behavior during cure (*i.e.*, changes in entanglements) [43], and forced solvent exclusion processes during chain extension and fibrillation can alter the adhesive behavior compared with nonsolvent containing materials. We have an ongoing program focused on exploring the impact of the solvent on the gel microstructure and resulting properties of these gels.

## Impact of Solvent Quality on Polybutadiene Gel Properties



Nominally, these solvent-swollen elastomers exhibit adhesive characteristics similar to pressure-sensitive and other low modulus elastomeric adhesives. First, the tack adhesion energies increase with decreasing temperatures due to an increase in the ability to dissipate energy. Second, the onset of fibrillation and extension during tack adhesion occurs in gels with a modulus less than $\sim 10^5$ Pa in the plateau region, similar to what is observed with pressure-sensitive adhesives. Third, reducing the gel crosslink density increases the extension during pull-off due to the process of cavitation and fibrillation, resulting in an increase in the practical work of adhesion. However, the presence of high solvent loadings in the gel will lead to interesting polymer-solvent miscibility effects which can alter the gel adhesion performance. For gels to perform at elevated temperatures a low volatility solvent is required. Two solvents that are suitable are dibutylphthalate (DBP) and bis(ethylhexyl) sebacate (BEHS). To qualitatively compare the polymer-solvent miscibility of BEHS and DBP in the polybutadiene based gels the polybutadiene networks were swollen in a variety of solvents with different solubility parameters. To perform the swelling experiments, the polybutadiene monomers were crosslinked without solvent. The network was then swollen at room temperature in the different solvents. Figure 6 shows the swelling results. The maximum network swelling occurs with solvents that have a solubility parameter near $18\,\mathrm{MPa}^{1/2}$. BEHS sits at the maximum in the swelling curve and exhibits higher swelling than DBP indicating that BEHS is a better solvent for this polybutadiene network.

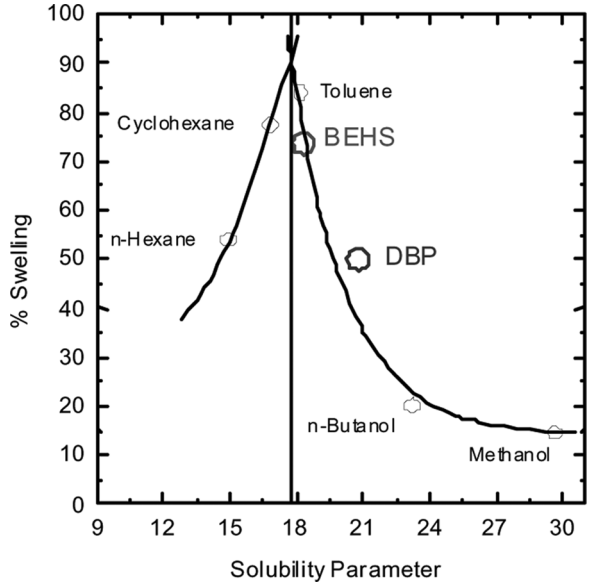


**FIGURE 6** Swelling experiments for the cured polybutadiene network in a variety of solvents with different solubility parameters.



Figure 7a compares the storage modulus-temperature profiles for MA5/R45 stoichiometric gels with either 60 mass% BEHS or 60 mass% DBP. The BEHS-based gel exhibits a glass transition temperature which is $\sim$25°C lower than the DBP-based gels. The storage modulus in the plateau region is similar for both the DBP and BEHS based gels. At these elevated temperatures, both DBP and BEHS are good solvents for the polybutadiene network. In addition, the cure temperature of 75°C for these gels is in a temperature regime where both solvents are miscible with the network, so the cured microstructure of the BEHS and DBP-based gels should be similar leading to a similar modulus value in the plateau region. Figure 7b shows the loss tangent data for the gels. The main peak in the loss tangent is due to the $T_g$ of the gel formulation. The DBP gel also exhibits a second peak in the loss tangent near $-85$°C. This corresponds to the glass transition temperature of DBP [44] and indicates phase separation at low temperatures with the DBP gel.

Polymer-solvent miscibility in the gel can impact the adhesive performance. Neutron scattering with deuterated DBP and deuterated BEHS showed that gels with 60 mass% DBP phase separate below 20°C, whereas gels with 60 mass% BEHS are fully miscible at

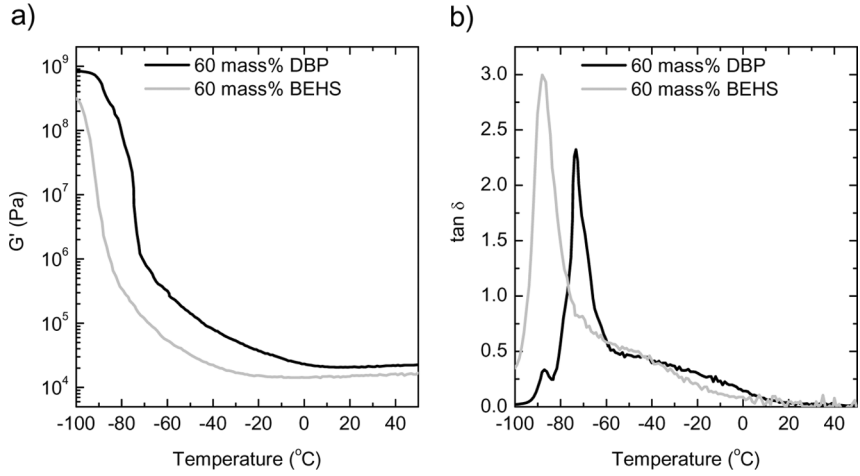


**FIGURE 7** Rheological data for an MA5/R45 stoichiometric gel formulation with either 60 mass% BEHS, or 60 mass% DBP, a) shear storage modulus as a function of temperature, and b) loss tangent as a function of temperature.



temperatures below −80°C. Figure 8 compares the tack adhesion energy for MA10/R45 stoichiometric and MA5/R45 stoichiometric formulations with either DBP or BEHS at a loading of 60 mass% solvent. The pull-off rate was 0.002 mm/s. Figure 8a shows the tack adhesion

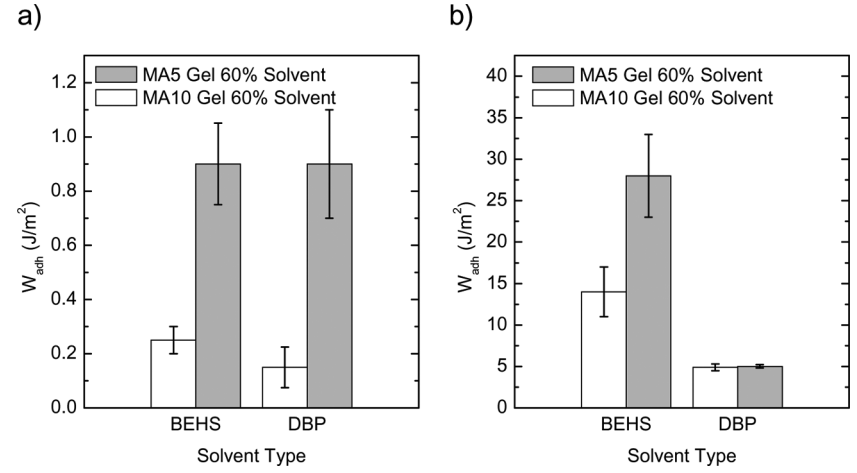


**FIGURE 8** Tack adhesion energy for MA10/R45 stoichiometric and MA5/R45 stoichiometric formulations with 60 mass% BEHS or 60 mass% DBP at a) 24°C and b) −60°C. The pull-off rate was 0.002 mm/s.

at 24°C. As shown previously, the MA10 gels had a higher crosslink density than the MA5 gel. For both solvents the lower crosslink density gel exhibited higher tack adhesion. Also, at room temperature (where both solvents are miscible with the polymer) the tack adhesion was independent of the solvent type. Figure 8b shows the tack adhesion at −60°C, where BEHS is miscible in the polymer, but DBP is not. The tack adhesion was much higher with the BEHS gels compared with the DBP-based gels at low temperatures. When the DBP-based gels phase separate at low temperatures a skin of solvent is likely excluded towards the gel surface, degrading the tack adhesion.

Solvent segregation issues can also have significant impact on other types of adhesion measurement techniques. Johnson-Kendall-Roberts (JKR)-based contact mechanics [27,45–47] is a common technique to assess adhesion of soft materials. Figure 9 shows a schematic of the JKR measurement process utilized in these experiments. Two hemispheres of polybutadiene gel (∼2 mm in diameter) were placed on separate glass slides. The two hemispheres are brought into contact with each other at a constant rate, while simultaneously measuring the load, displacement, and contact area between the two hemispheres.



Figure 10a plots displacement, $\delta$, as a function of loading force, P, for a typical JKR experiment. Both the loading and unloading curve are shown. As the displacement increases during the loading phase, the loading force also increases. Similarly, during the unloading phase, as the displacement decreases back towards the initial starting point of contact, the loading force also decreases. In this case, the hysteresis between the loading and unloading curve indicates an adhesive interaction at the interface between the two gel spheres. Fits to the JKR data are illustrated by the lines in Figure 10a, while the data are shown by the symbols on the graph. The fitting procedure was developed by Lin *et al.* [48]. Both the loading and unloading curves at room temperature were fit with a single modulus value, $E^*$, where $E^* = 4E/3 = 4G'$, E is the tensile modulus, and $G'$ is the gel shear storage modulus. The single modulus fit for both the loading and unloading curve indicates that bulk viscoelastic effects from the gel do not impact the JKR adhesion measurements. The modulus values obtained from the JKR measurements agree well with the values obtained from torsional rheology measurements on the same gel formulations. Table 1 shows the comparison of the JKR shear modulus value and the shear rheology modulus values for various gel formulations. For these experiments three different solvents were utilized including dodecane, DBP, and BEHS. Within the

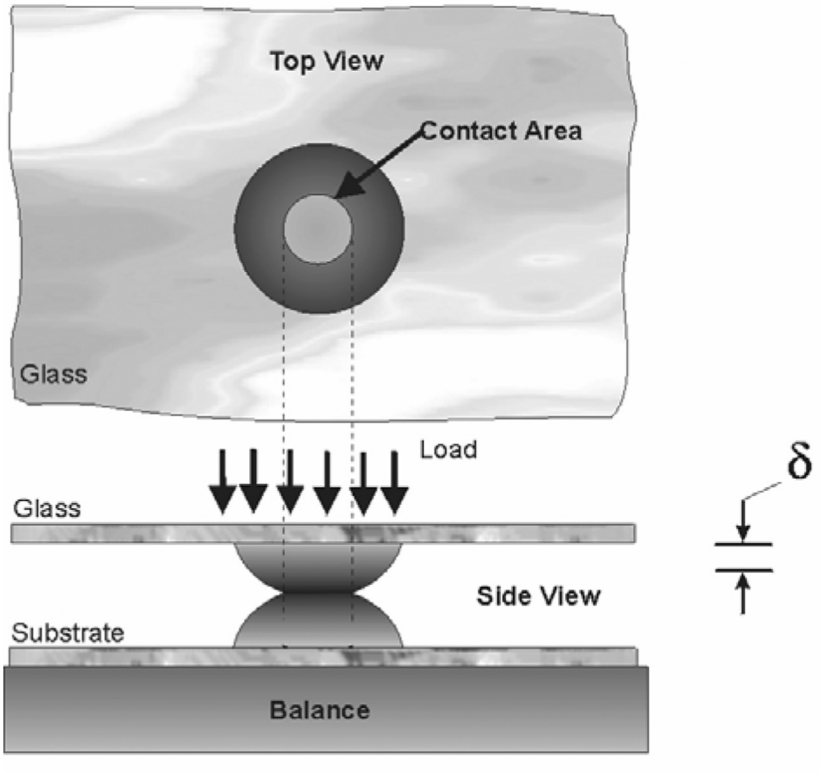


**FIGURE 9** A schematic of the JKR measurement technique utilized in these experiments.

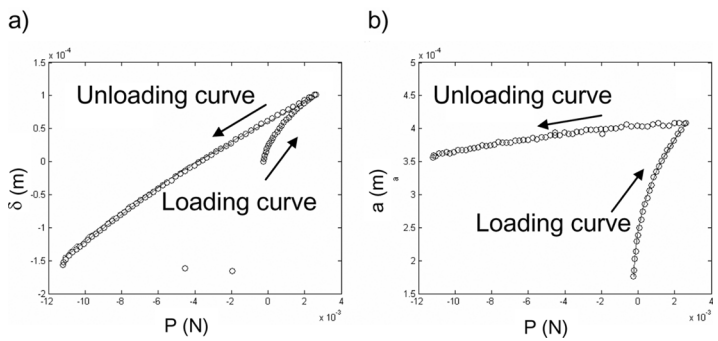


**FIGURE 10** a) Displacement as a function of load and b) contact area as a function of load for a typical JKR contact mechanics test on the polybutadiene gels. Both loading and unloading portions of the curves are shown.

**TABLE 1** Room Temperature Modulus Data Obtained for Various Gel Formulations through JKR and Torsional Rheology. The Error in the Modulus Values is ±10% and was Determined from Measurements on Multiple Samples

| Formulation | Solvent loading (mass %) | Solvent type | G′ (kPa) JKR | G′ (kPa) Torsional rheology |
|---|---|---|---|---|
| MA5/R45 stoichiometric | 40 | Dodecane | 43 | 46 |
| MA5/R45 stoichiometric | 40 | DBP | 36 | 43 |
| MA5/R45 stoichiometric | 40 | BEHS | 39 | 39 |
| MA10/R45 stoichiometric | 60 | BEHS | 119 | 105 |

experimental error (~10%) the modulus values from the two techniques are identical. The error was estimated from measurements on multiple samples of the same gel formulations.

Figure 10b plots the contact radius, a, as a function of loading force during the JKR measurement. Both the loading and unloading portions of the JKR experiment are shown. As the loading force increases during the loading portion, the contact area between the two gel hemispheres increases. During the unloading phase, as the loading force decreases, the contact area between the two hemispheres decreases. Utilizing the modulus values obtained from the force-displacement fit in Figure 10a, the loading portion of the contact area-load curve in Figure 10b was fit to obtain a single work of adhesion value, $W_{adh}$. Again, the fitting procedure is described by Lin *et al.* [48]. Table 2

**TABLE 2** Work of Adhesion Values ($J/m^2$) from JKR Measurement Compared with Calculated $W_{adh}$ Values from the Gel Formulation and Corrected $W_{adh}$ Values Based on the Assumption of Solvent Exclusion at the Hemisphere Interface During the JKR Measurement

| Formulation | Solvent loading (mass %) | Solvent type | JKR measured $W_{adh}$ | $2\gamma_{gel}$ $W_{adh}$ | $\theta$ (degrees) | $2\gamma_{solvent}\cos\theta$ $W_{adh}$ | Conclusion |
|---|---|---|---|---|---|---|---|
| MA5/R45 stoichiometric | 40 | Dodecane | 43.2 | 53.9 | 36.9 | 40.5 | Exclusion |
| MA5/R45 stoichiometric | 40 | DBP | 44.8 | 60.3 | 42 | 49.6 | Exclusion |
| MA5/R45 stoichiometric | 40 | BEHS | 61.2 | 58.4 | 48.3 | 41.2 | No exclusion |
| MA10/R45 stoichiometric | 60 | BEHS | 45.6 | 59.6 | 39.9 | 47.6 | Exclusion |

shows the JKR $W_{adh}$ values obtained for the stoichiometric MA5/R45 formulations with 40 mass% dodecane, DBP, or BEHS, and an MA10/R45 formulation with 60 mass% BEHS. Also shown in Table 2 are estimated work of adhesion values obtained from the thermodynamic definition that $W_{adh} = 2\gamma_g$ where $\gamma_g$ is the surface tension of the gel. For Table 2 the gel surface tension was estimated by a linear combination of the pure component surface tensions multiplied by the mass fraction of the component in the gel formulation. For the MA5/R45 gel with 40 mass% BEHS the JKR $W_{adh}$ agrees well with the estimated $W_{adh}$ value, calculated from the gel composition. For the MA5/R45 gel with either 40 mass% DBP or 40 mass% dodecane the JKR $W_{adh}$ value is significantly less than calculated based on the gel composition. The solubility parameter of dodecane is 16 $MPa^{1/2}$ and for DBP is 19.3 $MPa^{1/2}$. Swelling experiments showed that the gel exhibited a maximum in swelling with solvents that had a solubility parameter near 18 $MPa^{1/2}$. Therefore, both dodecane and DBP are less miscible in the crosslinked polybutadiene than BEHS. A potential explanation for the deviation of the JKR $W_{adh}$ from the calculated $W_{adh}$ based on the gel composition is that the solvent content at the hemisphere-hemisphere interface is not the same as in the bulk gel. This solvent exclusion could be intrinsic in the gel formulation due to preferential segregation of the solvent to the air interface or an exclusion process that occurs during the JKR measurement. The MA10/R45 sample with 60% BEHS also shows a difference between the measured and calculated values of the $W_{adh}$. The higher crosslink density and high solvent loading of this formulation makes it more susceptible to solvent exclusion effects, lending further credence to the hypothesis that solvent exclusion at the hemisphere interfaces is the cause of the lower JKR $W_{adh}$ values compared with the calculated values based on gel composition.

Research by Maugis [49] shows that JKR experiments in which the hemispheres are in the presence of a liquid meniscus leads to a $W_{adh}$ of $2\gamma_{liquid}\cos\theta$, where $\theta$ is the contact angle between the liquid and the gel formulation and $\gamma_{liquid}$ is the pure liquid surface tension. Table 2 also shows the advancing contact angles for the various solvents on a cured gel surface. $W_{adh}$ values, assuming a liquid meniscus and utilizing Maugis' result, agree well with the JKR measured $W_{adh}$ values for the MA5 gels with 40 mass% dodecane or DBP and for the MA10 gel with 60 mass% BEHS. However, Maugis' correction is not effective for predicting the JKR $W_{adh}$ for the MA5 formulation with 40 mass% BEHS. These results further support our hypothesis that solvent exclusion at interfaces can impact the adhesion results.

## Lightly Crosslinked Silicone Gels with High Extractables Content

Soft, lightly crosslinked silicone-based gels are also interesting materials with various applications where adhesion to a variety of substrates is critical. While, typically, solvents are not added to crosslinked silicone rubbers, the materials are qualitatively similar to polymer gels in that the extractables content is very high, 30% to 70%, in a typical commercially available silicone. The extractables content in silicone gels has a higher molecular weight when compared with the small molecule solvents added to the polybutadiene gel formulations. However, this sol content can impact the adhesion properties. The following data illustrates our active research in this area. Figure 11a shows a storage modulus-temperature profile for two soft silicone materials from Dow Corning. One, DC4–8022, is a typical silicone-oxygen-silicone backbone, having perfluoroalkyl pendant groups. The other is a random copolymer comprised of poly(dimethylsiloxane) and a poly(di-perfluoroalkylsiloxane), (monomer fraction of fluorinated silicone is $\sim 0.4$). The cure chemistry for both silicones involves crosslinking between vinyl and silane groups, accelerated with a platinum catalyst. Both silicone gels have a low storage modulus value in the plateau region (well below $10^5$ Pa) and should exhibit high tack adhesion with fibrillation and extension. The fluorinated silicone has



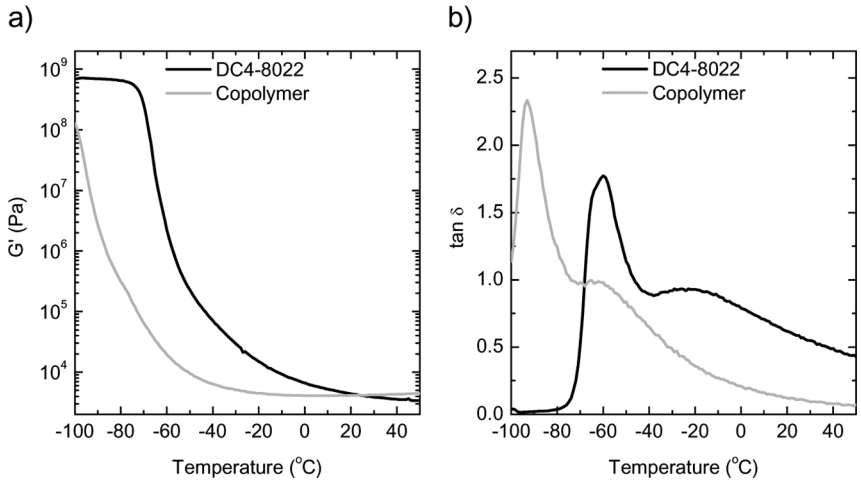


**FIGURE 11** Rheological data for the fluorinated silicone DC4–8022 and the copolymer silicone: a) storage modulus as a function of temperature and b) loss tangent as a function of temperature.

a glass transition temperature near −65°C, while the copolymer silicone exhibits at $T_g$ near −90°C. Typical poly(dimethylsiloxane) can have a $T_g$ below −100°C. The bulky fluorinated pendant group restricts the backbone mobility and raises the $T_g$ for these fluorinated materials. Figure 11b shows the loss tangent-temperature profiles for the same gel materials. Both silicone gels exhibit enhanced dissipation in the loss tangent spectrum near the glass transition temperature and, therefore, exhibit high tack adhesion values at low temperatures due to this enhanced energy dissipation. As was mentioned with the polybutadiene based gels, the molecular origin of the enhanced dissipation may be due to the presence of pendant chain defects in the gel structure. In addition, the large fraction of high molecular weight extractables in the silicone could contribute.

Figure 12a and 12b shows the tack adhesion stress-strain curves for the DC4–8022 at 24 and −30°C as a function of rate. Extension is observed at both temperatures and all rates. At 24°C the stress-strain curves are independent of the rate, which is consistent with the lower loss behavior of the silicone in the rubbery plateau region. However, at −30°C, strong rate dependence was observed due to a large increase in the stress maximum and increasing strain at final pull-off with increasing rate. This qualitatively correlates with the rising loss tangent value for the fluorinated silicone at −30°C.

Figure 13a shows the room temperature tack adhesion energy for the DC4–8022 as a function of rate. As was observed in the



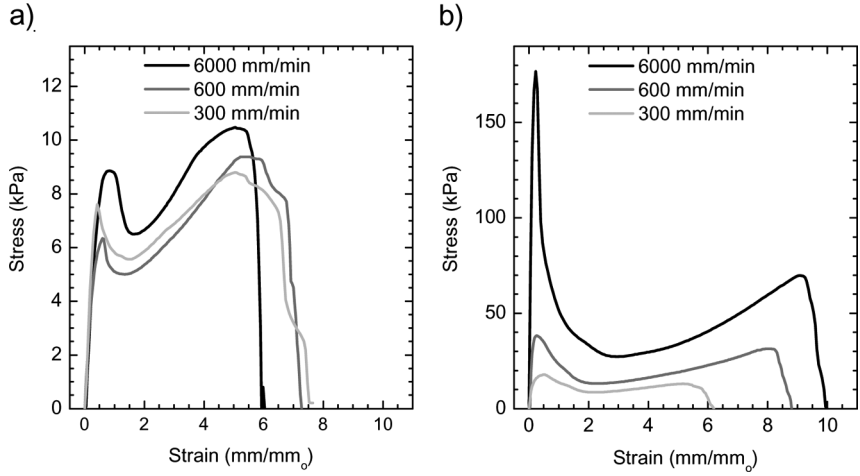


**FIGURE 12** Stress-strain tack adhesion curves for the fluorinated silicone DC4–8022 as a function of rate at a) 24°C and b) −30°C.

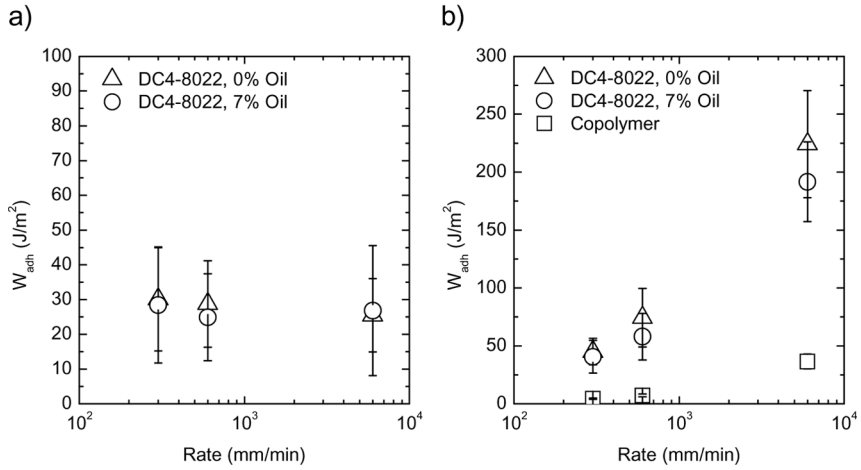


**FIGURE 13** Tack adhesion energy as a function of rate for the fluorinated silicone with and without the nonreactive oil, and the copolymer silicone at a) 24°C and b) −30°C.



stress-strain plots, the fluorinated silicone does not exhibit rate dependence at room temperature. Due to a limited supply of newly developed copolymer, tack adhesion was not measured with the copolymer at 24°C; however, due to the low loss behavior for the copolymer silicone at room temperature, we expect that no rate dependence will be observed in the copolymer tack adhesion measurements at that temperature. Figure 13b shows the −30°C tack adhesion as a function of rate for both silicones. The fully fluorinated material exhibits higher tack adhesion values and a stronger rate dependence than the copolymer, which is consistent with the higher loss tangent value for the DC4–8022. Similar to the polybutadiene-based gels, the silicone materials exhibit a qualitative correlation between the tack adhesion and the rheological loss tangent.

While silicone elastomers are not typically considered solvent-swollen, they are very much like a solvent-swollen gel because the commercial silicones can have substantial extractable/unreacted material in the formulation. One major difference between the silicone gels and polybutadiene gels is that the solvent in the polybutadiene gels is a small molecule that can diffuse fairly rapidly through the gel material. For soft silicone gels the extractables can be high molecular weight silicone chains that diffuse through the network more slowly. This could lead to an adhesive aging problem with the silicone materials due to the potential for the nonreactive chains to segregate

gradually towards critical interfacial regions and degrade the adhesion. The fluorinated silicone DC4–8022 in Figure 11 has a neat extractables content near 60 mass% depending on the incoming material hardness. To further test the impact of extractables on the silicone adhesion, 7 mass% of a nonreactive fluorinated silicone oil was mixed with the commercial DC4–8022 silicone. The nonreactive silicone oil has a molecular weight of 10,000 g/mole which is within a typical range for extractables in a soft silicone. The silicone oil also matches the backbone chemistry of the DC4–8022; however, it contains no reactive functional groups and can not tie into the crosslinked network. Figure 13 also shows the tack adhesion energy for the fluorinated silicone with 7% of the nonreactive oil added to the formulation. The tack adhesion energies were not significantly affected by the addition of this oil content. In addition, no significant changes were observed in the stress-strain curves due to the presence of the oil. Our concern regarding extractables is the potential long-term aging performance of adhesive bonds. If the nonreactive extractables segregate towards interfaces gradually with long-term aging, then the adhesion can be degraded leading to device failures. While the presence of excess extractables in the 7% oil formulation does not impact the initial tack adhesion, it may impact the adhesive aging. A long-term aging study is currently underway to probe the impact of adhesive aging as a function of the silicone gel extractables content. The existing stress condition in a polymer gel could impact the adhesive aging phenomena, as segregation of sol material to critical interfaces could be accelerated with a stress field. Generally, the best way to test this impact is with practical devices where the gel is in the natural environment and stress state for the application. However, we are also engaged in a fundamental program to investigate the solvent exclusion phenomenon in gel materials. In addition to the stress conditions, the molecular weight, extent of branching, and chemical functionality of the sol material as well as the crosslink density of the gel will impact this phenomenon.

Tack can probe the ability of a material to dissipate energy. However, it does not include contributions due to a strengthened interface that can occur when a gel is cured in the presence of a substrate. Peel adhesion measurements, where the gel is sandwiched between two substrates and cured in the presence of the substrate, is a technique more suited for this type of analysis. For peel experiments with the DC4–8022 the substrate was an aluminum-Mylar laminate structure. The fluorinated silicone gel was sandwiched between two sheets of laminate with either both aluminum faces or both Mylar faces of the laminate in contact with the silicone. The silicone was then cured in

contact with either the aluminum or Mylar. The thickness of the gel layer was controlled by utilizing 0.25 mm (10 mil) shimstock as a spacer between the laminate structure. The surfaces of the laminate were cleaned by a gentle wipe with an isopropanol soaked rag, followed by 30 s exposure to UV-ozone cleaner, before depositing the silicone on the substrate. Figure 14a shows the peel force at 24°C for the fluorinated silicone gel sandwiched between two Mylar (MGM) substrates or two aluminum substrates (AGA) as a function of the peel rate and the extractables content in the formulation. Figure 14b shows data for similar samples at −60°C. Similar to the tack adhesion results for both the polybutadiene gels and the silicone, the peel adhesion force increases with the decreasing peel temperature and increasing peel rate. As expected, based on the increased energy dissipation of the gel at −60°C, the rate dependence on the peel adhesion is stronger at −60°C than at 24°C. The peel forces for the AGA samples are higher than for the MGM samples and the AGA samples show stronger rate dependence than the MGM samples at both 24 and −60°C.

The failure mechanism provides insight into the differences between the MGM samples and the AGA samples. At both temperatures with the MGM samples the silicone failed adhesively during peel at the Mylar-gel interface. For the AGA samples, however, the failure mechanism was cohesive in the bulk silicone gel, leaving a thin layer



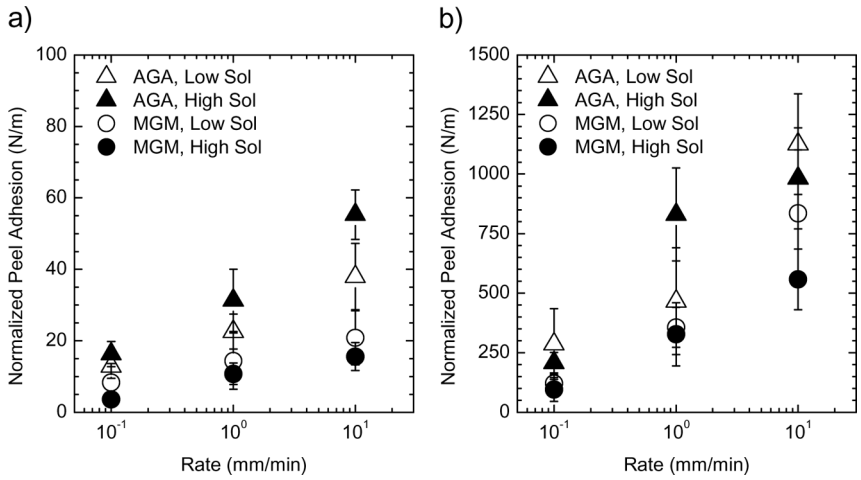


**FIGURE 14** Peel adhesion measurements for the DC4–8022 silicone gel with no oil (low sol) and 7% nonreactive oil (high sol) added to the formulation between aluminum or Mylar substrates at temperatures of a) 24°C and b) −60°C.

of gel on both aluminum surfaces. For the MGM samples the interface between the silicone and the Mylar is weaker than the interface between the aluminum and the gel in the AGA samples. This means that stress is not transferred as effectively to the bulk gel material in the MGM samples and the energy dissipating mechanisms in the gel do not play as strong a role in the peel measurement. This causes lower peel force values and a smaller rate dependence in the MGM samples compared with the AGA samples. The stronger interaction between the gel and the aluminum could be caused by a number of mechanisms. Atomic force microscopy (AFM) images of both the Mylar and aluminum surfaces showed approximately the same (RMS) roughness of $\sim$15 nm. However, the native aluminum oxide layer on aluminum can often be porous on a molecular scale. This molecular level porosity would not be detected with the AFM images; however, it could lead to a significantly higher contact area with the gel and mechanical interlocking on a molecular level that would dramatically strengthen the interface. Another possible factor is that the aluminum is a higher energy surface. The higher surface energy of the aluminum would lead to a stronger thermodynamic work of adhesion with the gel in contact with the aluminum. If this thermodynamic work of adhesion is sufficiently strong, then stress could be transferred to the bulk material more effectively in the AGA samples. A final explanation is that the silicone may chemically react with native hydroxyl groups on the aluminum oxide surface leading to covalent bonds at the interface that will strengthen the adhesion. Chemical bonding between silanol and siloxane groups has been utilized to explain adhesion hysteresis for polydimethylsiloxane adhered to glass surfaces [50]. The initial peel adhesion values were not impacted by adding 7% of the nonreactive oil. However, this could change with long-term aging due to a gradual segregation of the oil/extractable material to the gel interfacial region. This potential aging issue is particularly relevant in light of past research on the impact of interfacial slippage on peel adhesion measurements [51]. Slippage of an elastomeric adhesive was more pronounced on higher mobility surfaces, leading to a decrease in the measured peel forces. Interfacial segregation of small molecular weight extractables in the silicone gels could enhance this slippage mechanism.



## CONCLUSIONS

Tack, JKR, and peel adhesion measurements were utilized to characterize the adhesive properties of polymer gels. Nominally these solvent swollen materials exhibit adhesive characteristics similar to nonsolvent

swollen elastomers including: (1) an increase in tack adhesion energies with increasing pull-off rates and decreasing temperatures in the rubbery region, (2) qualitative correlation between the rheological loss tangent for the gel and the gel adhesion energy, (3) fibrillation and extension during adhesion testing for gels with a shear modulus value less than $10^5$ Pa in the plateau region, and (4) a decrease in the adhesion energy with increasing crosslink density. However, interfacial solvent exclusion effects can degrade the adhesive properties of these soft materials. These exclusion effects must be considered for accurate interpretation of adhesion data and intelligent design of gel materials for practical applications.

## ACKNOWLEDGEMENTS

The authors would like to thank Scott Campin, Shannon Lacy, Ron Sanchez, Duane Schneider, John Schroeder, Gayle Schwartz, Scott Spangler, and Jason Tillotson for assistance in sample preparation and data acquisition. Collaboration with Ann Norris of Dow Corning is gratefully acknowledged for assistance with the design of the silicone-based gels. This work was performed at Sandia National Laboratories. Sandia is a multiprogram laboratory operated by Sandia Corporation, a Lockheed Martin Company, for the United States Department of Energy's National Nuclear Safety Administration under contract DE–AC04–94AL85000.



## REFERENCES

[1] Wu, S., *Polymer Interface and Adhesion* (Marcel Dekker, Inc., New York, 1982).
[2] Brown, H. R., *IBM J. Res. Dev.* **38**, 379–389 (1994).
[3] Brown, H. R., *Macromolecules* **34**, 3720–3724 (2001).
[4] Schnell, R., Stamm, M., and Creton, C., *Macromolecules* **32**, 3420–3425 (1999).
[5] Brown, H. R., *Macromolecules* **22**, 2860–2863 (1989).
[6] Dai, C.-A., Dair, B. J., Ober, C. K., Kramer, E. J., Hui, C.-Y., and Jelinski, L. W., *Phys. Rev. Lett.* **73**, 2472–2475 (1994).
[7] Washiama, J., Kramer, E. J., and Hui, C.-Y., *Macromolecules* **26**, 2928–2934 (1993).
[8] Brown, H. R., *Macromolecules* **26**, 1666–1670 (1993).
[9] Brown, H. R., Hui, C.-Y., and Raphael, E., *Macromolecules* **27**, 608–609 (1994).
[10] Gent, A. N. and Schultz, J., *J. Adhes.* **3**, 281 (1972).
[11] Andrews, E. H. and Kinloch, A. J., *Proc. R. Soc. (London)* **A332**, 385–399 (1973).
[12] Williams, M. L., Landel, R. F., and Ferry, J. D., *J. Am. Chem. Soc.* **77**, 3701–3707 (1955).
[13] Dusek, K. (ed.), *Responsive Gels: Volume Phase Transitions, Advances in Polymer Science* (Springer, Berlin, 1993).
[14] Flory, P. J., *Principles of Polymer Chemistry* (Cornell University Press, Ithaca, NY, 1953).

[15] de Gennes, P. G., *Scaling Concepts in Polymer Physics* (Cornell University Press, Ithaca, NY, 1979).
[16] Tanaka, T., *Phys. Rev. Lett.* **40**, 820–823 (1978).
[17] Hamlen, R. P., Kent, C. E., and Shafer, S. N., *Nature* **206**, 1149–1150 (1965).
[18] Steinberg, I. Z., Oplatka, A., and Katchalsky, A., *Nature* **210**, 568–571 (1966).
[19] Kwon, I. C., Bae, Y. H., and Kim, S. W., *Nature* **354**, 291–293 (1991).
[20] Miyata, T., Asami, N., and Uragami, T., *Nature* **399**, 766–769 (1999).
[21] Murdan, S., *J. Controlled Release* **92**, 1–17 (2003).
[22] Peppas, N. A., Huang, Y., Torres-Lugo, M., Ward, J. H., and Zhang, J., *Annu. Rev. Biomed. Eng.* **2**, 9–29 (2000).
[23] Irvin, D. J., Goods, S. H., and Whinnery, L. L., *Chem. Mater.* **13**, 1143–1145 (2001).
[24] Kubota, N., Watanabe, H., Konaka, G., and Eguchi, Y., *J. Appl. Polym. Sci.* **76**, 12–18 (2000).
[25] Abraham, K. M. and Alamgir, M. J., *Power Sources* **43**, 195–208 (1993).
[26] Gent, A. and Petrich, R., *Proc. R. Soc. (London)* **A310**, 433–448 (1969).
[27] Shull, K. R., *Mater. Sci. Eng. R.* **36**, 1–45 (2002).
[28] Lakrout, H., Sergot, P., and Creton, C., *J. Adhes.* **69**, 307–359 (1999).
[29] Zosel, A., *J. Adhes.* **30**, 135–149 (1989).
[30] Zosel, A., *J. Adhes.* **34**, 201–209 (1991).
[31] Zosel, A., *Int. J. Adhes. & Adhesives* **18**, 265–271 (1998).
[32] MA5, MA10, and R45 were obtained from Sartomer. See Sartomer product sheets at www.sartomer.com.
[33] Billmeyer, Jr., F. W., *Textbook of Polymer Science* (John Wiley & Sons, New York, 1984).
[34] Girard-Reydet, E., Oslanec, R., Whitten, P., and Brown, H. R., *Langmuir* **20**, 708–713 (2004).
[35] Dalquist, C. A., in *Treatise on Adhesion and Adhesives*, Patrick, R. L. (Ed.) (Dekker, New York, 1969), Vol. 2.
[36] Creton, C. and Leibler, L., *J. Poly. Sci. B Poly. Phys.* **34**, 545–554 (1996).
[37] Hui, C.-Y., Lin, Y. Y., Baney, J. M., and Kramer, E. J., *J. Poly. Sci. B Poly. Phys.* **39**, 1195–1214 (2001).
[38] de Gennes, P. G., *Langmuir* **12**, 4497–4500 (1996).
[39] Lakrout, H., Creton, C., Ahn, D., and Shull, K. R., *Macromolecules* **34**, 7448–7458 (2001).
[40] Creton, C., Hooker, J., and Shull, K. R., *Langmuir* **17**, 4948–4954 (2001).
[41] Brown, K., Hooker, J. C., and Creton, C., *Macromol. Mater. Eng.* **287**, 163–179 (2002).
[42] Gay, C. and Leibler, L., *Phys. Rev. Lett.* **82**, 936–939 (1999).
[43] Sivasailam, K. and Cohen, C., *J. Rheol.* **44**, 897–915 (2000).
[44] Wang, L.-M., Velikov, V., and Agnell, C. A., *J. Chem. Phys.* **117**, 10184–10192 (2002).
[45] Johnson, K. L., Kendall, K., and Roberts, A. D., *Proc. R. Soc. (London)* **A324**, 301–313 (1971).
[46] Ahn, D. and Shull, K. R., *Macromolecules* **29**, 4381–4390 (1996).
[47] Flanigan, C. M. and Shull, K. R., *Langmuir* **15**, 4966–4974 (1999).
[48] Lin, Y. Y., Hui, C.-Y., Cole, P. J., Lenhart, J. L., and Emerson, J. A., *Proc. Adhes. Soc.* **1**, 60 (2004).
[49] Maugis, D. and Gauthiermanuel, B., *J. Adhes. Sci. Technol.* **8**, 1311–1322 (1994).
[50] Toikka, G., Spinks, G. M., and Brown, H. R., *J. Adhes.* **74**, 317–340 (2000).
[51] Newby, B. Z., Chaudhury, M. K., and Brown, H. R., *Science* **269**, 1407–1409 (1995).